Virginia Commonwealth University
VCU Scholars Compass

Theses and Dissertations | Graduate School

2011

INDUCING ACTIVE SITES IN CLUSTERS: REACTIVITY OF Al13Ix- and Al14Iy- (x=0-2, y=2-4) WITH METHANOL

Christopher Powell
Virginia Commonwealth University

Follow this and additional works at: https://scholarscompass.vcu.edu/etd

 Part of the Physics Commons

© The Author

Downloaded from
https://scholarscompass.vcu.edu/etd/213

This Thesis is brought to you for free and open access by the Graduate School at VCU Scholars Compass. It has been accepted for inclusion in Theses and Dissertations by an authorized administrator of VCU Scholars Compass. For more information, please contact libcompass@vcu.edu.

www.manaraa.com

INDUCING ACTIVE SITES IN CLUSTERS:

REACTIVITY OF $Al_{13}I_x^-$ and $Al_{14}I_y^-$ ($x = 0-2$, $y = 2-4$) WITH METHANOL

A thesis submitted in partial fulfillment of the requirements for the degree of Master of Science in Physics at Virginia Commonwealth University

by

CHRISTOPHER L. POWELL

B.S. in Physics and Mathematics

Virginia Commonwealth University, 2009

M.S. in Physics

Virginia Commonwealth University, 2011

Director: SHIV KHANNA

COMMONWEALTH PROFESSOR, DEPARTMENT OF PHYSICS

www.manaraa.com

Acknowledgement

I owe the utmost appreciation to Dr. Shiv Khanna for his generous advisement and assistance over the past two years. His depth of knowledge, creativity, and work ethic has greatly inspired me as I have pursued my degree. I would like to thank the entire Khanna Research Group, in particular Dr. Arthur Reber and S. Vincent Ong. Art and Vince have spent so much time answering my innumerable questions with patience and understanding that it is hard to imagine how they got their own work done, and I could not have done this without their help. I would like to acknowledge the assistance of the Air Force Office of Scientific Research [AFOSR], FA9550-09-1-0371.

I would like to express my thanks for the endless support offered to me by my parents, Mark and Karen. They take every opportunity to encourage me and brag to their friends, and that has played a large part in motivating me to this point. I would like to thank my roommates over the past two years, first my brother Trent and now my good friend Jason, who have been there to support me day in and day out. Lastly, my girlfriend Jenny, who has done more than her fair share to keep me sane and focused over the past two years, has my absolute gratitude.

www.manaraa.com

Table of Contents

www.manaraa.com

List of Figures

www.manaraa.com

www.manaraa.com

Abstract

Size selective reactivity has been observed in pure aluminum cluster anions as a result of Lewis acid and base pairs. Using this a starting point, the goal of this study has been to explore how reactivity is affected with the addition of one or more ligand, which may induce active sites on the surface of the metal clusters. To study this, a theoretical investigation was undertaken on $Al_{13}I_x^-$ and $Al_{14}I_y^-$ ($x = 0-2, y = 2-4$) and their reactivity with methanol. The hypothesis was that iodine can induce a Lewis base site on the opposite side of the cluster, which may enhance reactivity.

In results that are consistent with preliminary experimental data, it was found that the $Al_{13}I_x^-$ series has a large energy barrier with respect to the cleavage of the O-H bond of methanol. The clusters of the series act as an extremely poor Lewis acids, and as a result, these clusters are relatively inert to methanol etching. On the other hand, the $Al_{14}I_y^-$ series has a low barrier and is expected to react rapidly with methanol. The series is found to be most reactive at an aluminum adatom that is bound to an iodine due to the iodine extracting charge from the aluminum cluster creating a strong Lewis acid site.

www.manaraa.com

Chapter 1, Introduction

1.1, Background

The quantum chemical investigation of clusters containing two to a few hundred atoms has grown in prominence in past decades, beginning as an approach to address consistent anomalies in mass spectra results of cluster distributions[1,2]. Cluster science has evolved into an exciting field encapsulating the investigation of electronic, physical, and chemical properties of systems in the scale of nanometers or smaller. Of particular interest to this study is the emerging concept of the "superatom". Superatoms are clusters of atoms that have the same effective valence as specific elements, mimicking their behaviors[1]. The "superatom" designation arrives from the concept of a closed electronic shell, which may be thought of as the zero valence of the cluster. In metallic clusters, electronic shell closure may be understood under consideration of what is known as the jellium model. Within this model, a positive charge representing the nuclei and bound electrons is uniformly distributed over a sphere the size of the particular cluster[2]. The valence electrons move as a nearly free electron gas around this positive core, forming shells, or "supershells", with occupancies and vacancies comparable to atomic orbitals. Such electrons have energy levels grouped into "supershells", $1s^2$, $1p^6$, $1d^{10}$, $2s^2$, $1f^{14}$, $2p^6$, etc, which correspond to the electronic shells of an individual atom[3]: $1s^2$, $2s^2$, $2p^6$, $3s^2$, $3p^6$, $4s^2$, $3d^{10}$, etc. (Fig. 1).

www.manaraa.com

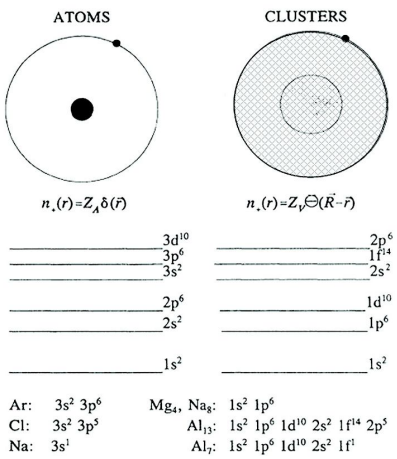

Fig. 1, Energy levels for atoms and clusters[2].

Support for this model is seen in numerous experiments measuring electron affinity, ionization potential, and reactivity as demonstrated by the Castleman group at Pennsylvania State University[3]. Those studies addressed the observation that Al_x^- ($x = 13, 23, 37$) were relatively nonreactive compared to other aluminum cluster anions when exposed to oxygen. Aluminum has three valence electrons, meaning that the number of free electrons in an anionic cluster of N aluminum atoms is 3N+1. The mass abundances could thus be explained by lack of reactivity due to shell closings at 40, 70, and 112 electrons, which are predicted by the jellium model and seen in the mass spectra of simple metal clusters.

Studying the reactivity of matter of this size regime can give insight into the relationship between geometric structure, electronic properties, and chemical behavior[4]. Furthermore, studying individual clusters of selected size allows for the investigation of the fundamental factors that control the chemical reactivity of those clusters and helps identify mechanisms which govern all chemical reactivity at size regimes of the nano and subnanoscale. Studies of this type are of interest because clusters, particularly

www.manaraa.com

superatoms, which can be regarded as forming a third dimension to the periodic table of the elements by mimicking certain elements, are potentially tunable and thus could be developed as building blocks for bulk materials with highly controllable properties such as magnetism, band gap, and reactivity[2]. The physical production of cluster-assembled materials has several inherent challenges that lay ahead, such as determining the rules that would govern their properties and assembly[5]. However, a necessary preliminary step is exploring reactivity and other molecular characteristics of the free clusters that would constitute such a material.

1.2, Motivation

The reactivity of aluminum cluster anions, Al_x^- ($x = 7-18$), with H_2O, or water, has been explored[6], and the results show that some clusters with open electron shells experience no significant reactivity while some clusters with closed electronic sub-shells are found to be highly reactive. This is the opposite result as expected from reactivity studies with molecular oxygen, in which clusters with closed electronic shells are resistant to reactivity, while all cluster with open electronic shells are highly reactive[10]. Further investigation led to the determination that these behaviors have geometric origin resulting from uneven charge distribution. Spherical metallic clusters are expected to have an even distribution of charge around their surface. However, clusters are generally not spherical, but instead their shapes are distorted due to so-called Jahn-Teller distortions[7], which are a consequence of incomplete electronic shells. The result of the typical non-spherical nature, in which there is often one or more defect on a geometrically stable core, is that such a cluster will have an uneven charge distribution on

www.manaraa.com

its surface[6]. Then a particular site of a cluster will accept or donate electrons in a manner that is unique relative to other sites. Then, it has been found that the tendency towards charge transfer at different sites greatly determines the reactivity of aluminum cluster anions with water. The nucleophilic characteristic of water, meaning that it donates electrons in a reaction, makes the reactivity of it with aluminum clusters depend greatly on the Lewis acidity of different cluster sites. Here, a Lewis acid accepts a pair of electrons from the H_2O while a Lewis base donates an electron-pair resulting in an adduct[8]. The results of the study of water and aluminum cluster anions suggest that the reactivity which results from the existence of a Lewis acid and base in close proximity, and the O-H bond is split due to the relatively small distance between the two[6].

Thus, size selective reactivity has been observed in pure aluminum cluster anions as a result of the existence of geometrically close Lewis acid and base pairs, or complementary active sites. Of interest is how reactivity is affected with the addition of one or more ligands, which may induce active sites on the surface of the metal clusters. To study this, a theoretical investigation was undertaken on $Al_{13}I_x^-$ and $Al_{14}I_y^-$, where $x = 0-2$ and $y = 2-4$, and their reactivity with CH_3OH, or methanol. Iodine was chosen as the ligand based on a published study of the reactivity of $Al_{13}I_x$- and $Al_{14}I_y$- with O_2[10] as well as preliminary experimental data from the Castleman group on the reactivity of $Al_{13}I_x$- and $Al_{14}I_x$- with methanol. The hypothesis behind this study is that the addition of uncharged iodine to an aluminum cluster anion can induce a Lewis base site on the opposite side of the cluster, which may enhance reactivity.

For the purpose of this study, methanol was used to probe the reactivity behavior of the aluminum iodide cluster anions. This is related to the aforementioned study of

www.manaraa.com

pure aluminum anions with water because, as in water, the O-H bond in methanol is nucleophilic. Thus, methanol is expected to react with aluminum cluster anions in a manner chemically similar to water. Indeed, experimental and theoretical results have shown that the reactivity patterns of pure aluminum cluster anions of various sizes with water and methanol are very similar[29]. An important difference between the two is that methanol has a lower vapor pressure than water, so adding methanol to a system is comparable to adding boiling water. Methanol is more reactive than water, since the O-H bond in methanol breaks slightly more easily, so methanol is more prone to etching. This means that when methanol is added to an aluminum cluster for example, it may react, resulting in O-H bond cleavage. Eventually, enough energy is released so that individual aluminum atoms may be ripped from the cluster, continuing until the cluster reaches a closed shell character. Since methanol is more reactive, if a cluster survives methanol it will survive water.

1.3, Experimental Basis

The presented results have experimental basis in the work of the research group directed by Will Castleman at Pennsylvania State University. In one article, published in Science in 2005[10], pure aluminum cluster anions were reacted with I_2 gas, and then the aluminum iodide anions were etched by O_2. The following figure includes the mass spectra of the pure aluminum anions and of the aluminum iodide cluster anions:

www.manaraa.com

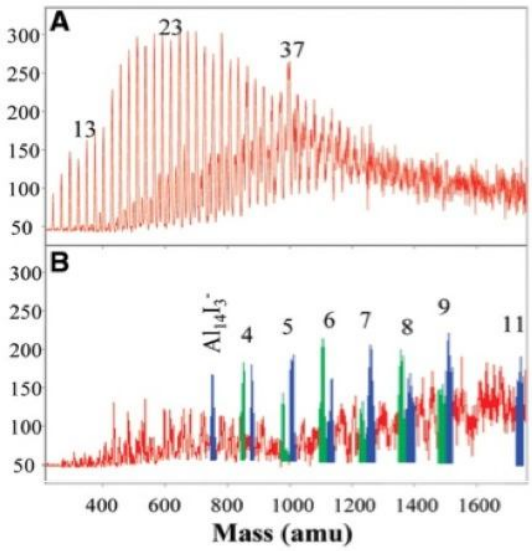

Fig. 2, Mass spectra of (A) Al cluster anions (B) reacted with I_2 vapor at high concentrations. The *y*-axis is peak intensity in arbitrary units[10].

Here the green peaks are of the $Al_{13}I_x^-$ series, and the blue are of the $Al_{14}I_y^-$ series. Firstly, Al_{13}^-, with an atomic mass of 351 amu, is present in Fig. 2b with the other pure aluminum anions, but when I_2 is introduced it is etched away, with no corresponding prominent peak in Fig. 1b. In fact, no prominent peaks from the $Al_{13}I_x^-$ series appear below $x = 4$, suggesting that relatively few $Al_{13}I_x^-$ are formed when aluminum cluster ions are combined with I_2 when $x = 0 - 2$. Similarly, the first prominent peak of the $Al_{14}I_y^-$ series occurs for $y = 3$. In the same study, a mass spectrum was produced for aluminum iodide cluster anions when I_2 was added at a very low concentration regime. The following figure has been adapted to highlight clusters of interest:

www.manaraa.com

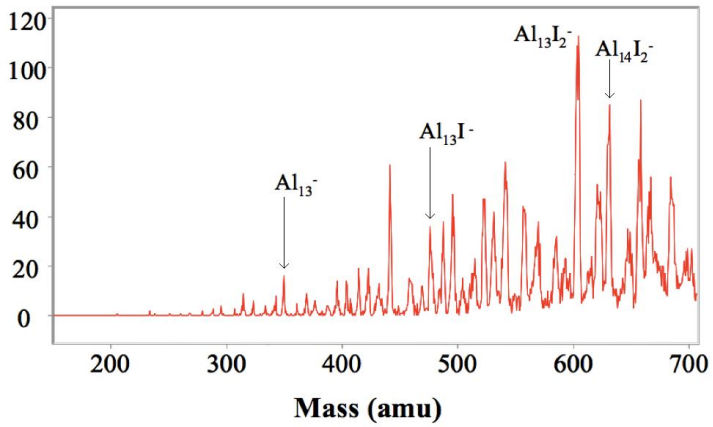

Fig. 3, Mass spectrum of Al cluster anions reacted with I_2 vapor in very low concentrations. The *y*-axis is peak intensity in arbitrary units[10].

Then in the case of very low concentrations of I_2 being added to aluminum cluster anions in the same experimental setup, a more prominent peak develops for $Al_{13}I_x^-$ where $x = 2$ but not for $x \leq 1$. Note that peaks for $Al_{14}I_y^-$ ($y = 3,4$) are not visible because those cluster anions have atomic masses of 759 and 886 amu respectively.

In a preliminary study performed in the same manner by the Castleman group, the following aluminum iodide mass spectrum was generated:

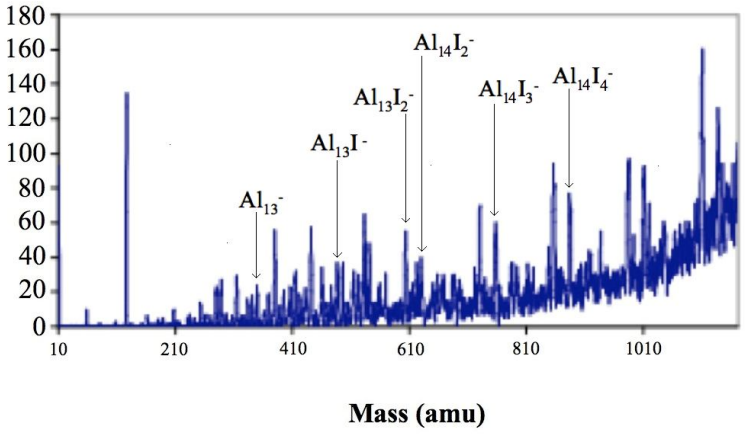

Fig. 4, Mass spectrum of Al cluster anions reacted with I_2 vapor. The *y*-axis is peak intensity in arbitrary units.

www.manaraa.com

Here there are pairs of peaks, beginning distinctly at 605 amu with $Al_{13}I_2^-$, with 27 amu between the peaks and 127 amu from pair to pair. In each case, the leftmost peak is of the $Al_{13}I_x^-$ series, and the rightmost is of the $Al_{14}I_y^-$ series. The peaks are separated by 27 amu as that is the atomic mass of aluminum, and the pairs are separated by 127 amu as that is the atomic mass of iodine. Here, as in Fig. 2, $Al_{13}I_x^-$ ($x = 0, 1$) do not show distinct peaks, again suggesting that relatively few of these species are formed when aluminum cluster ions are combined with I_2. In this experiment the aluminum iodide cluster anions were introduced to methanol, which produced the following mass spectrum:

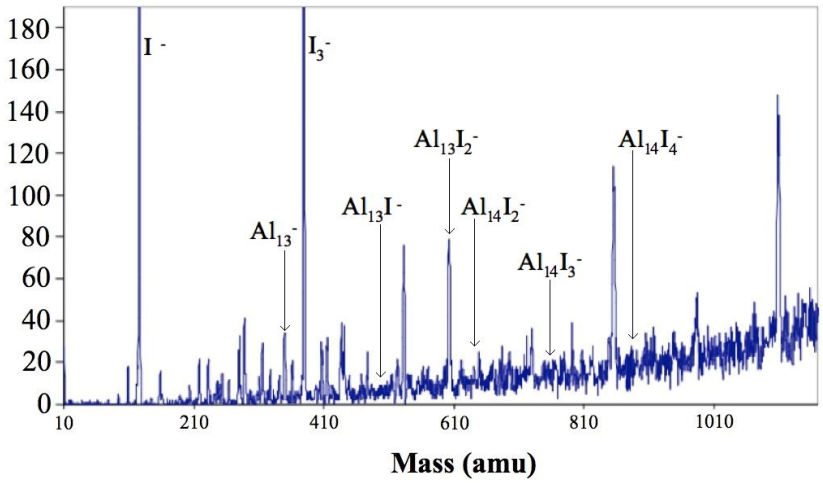

Fig. 5, Mass spectrum of aluminum iodide cluster anions etched by CH_3OH. The *y*-axis is peak intensity in arbitrary units.

The original spectrum contains numerous aluminum iodide cluster anions of all sizes, but after the addition of methanol, Al_{13}^- and $Al_{13}I_2^-$ is all that is abundant of those species of interest. The results are inconclusive for $Al_{13}I^-$ reacted with methanol, since there was not much to begin with (Fig. 4). It should be noted that peaks representing $Al_{13}I_3^-$ and $Al_{13}I_5^-$ seem visible in spectrum, with atomic masses of 732 and 859 amu respectively.

www.manaraa.com

All clusters of interest from the $Al_{14}I_y^-$ series have been etched away. The high numbers of I^- and I_3^- suggest that the introduction of methanol caused fragmentation of the I_2 that had been attached to aluminum clusters.

The experimental setup utilized to produce each of the described mass spectra results was a fast-flow tube apparatus[9] with a laser source used to ablate substances of interest[10]. In this case, the laser source vaporized an aluminum rod under translation and rotation in the presence of helium gas. The vaporized aluminum was cooled to the temperature of the sides of its container, room temperature, and exposed to gaseous I_2 at a controlled rate. For the methanol stage, described in Fig. 5, the steps were repeated, but after the I_2 reaction CH_3OH was introduced to the mixture at a controlled rate. In all cases, product clusters were sampled through a single-millimeter extraction orifice and analyzed using quadrupole mass spectrometry, a technique which removes neutral clusters.

In this project, theoretical methods are used to examine the reaction pathways between methanol and $Al_{13}I_x^-$ and $Al_{14}I_y^-$ ($x = 0-2$ and $y = 2-4$) with the intention of identifying the effect of iodine ligands on the reactivity. The hypothesis behind this study is that iodine may perturb the electronic structure of the metallic cluster which may result in the induction of a Lewis acid on the opposite side of the cluster, with the hope that this would affect reactivity. Size-selective reactivity has been observed in preliminary experiments, which validates the determination that these clusters are of interest. By identifying the sites at which the methanol reacts with these clusters, and their relative transition state, binding, and reaction energies, we hope to identify the way in which iodine ligands affect the reactivity of aluminum clusters.

www.manaraa.com

Chapter 2, Theory

2.1, Development of Numerical Methods for Solving the Schrödinger Equation

The fundamental problem of chemistry and physics at the quantum scale often takes the form of finding the solution of the time-independent Schrödinger equation for some particular quantum system.

$$\hat{H}\Psi = E\Psi \,. \tag{1}$$

This equation describes all properties of such a system, and thus serves as the foundation for all of quantum mechanics. It is comprised of the Hamiltonian operator ($\hat{H}$), the energy (E), and the total wave function (Ψ), a function of the spin and position of each electron. The time-independent Schrödinger equation takes the following full form:

$$\hat{H}\Psi = \sum_{i=1}^{N}\left(-\frac{\hbar}{2m}\nabla_i^2\Psi - Ze^2\sum_{\vec{R}}\frac{1}{\left|\vec{r}_i - \vec{R}\right|}\Psi \right) + \frac{1}{2}\sum_{i\neq j}\frac{e^2}{\left|\vec{r}_i - \vec{r}_j\right|}\Psi = E\Psi \,, \tag{2}$$

where i and j represent the i -th and j -th electron respectively, $\vec{r}$ represents the electron position, and $\vec{R}$ represents the nucleus position. The Hamiltonian operator is comprised of three terms, one each representing the following: the summed kinetic energy of each of N electrons, the summed potential energy due to positive electrostatic potential of each nucleus, and the Coulombic interaction between each electron. There is not a kinetic energy term for the nuclei because, according to the adiabatic approximation, since nuclei move very slowly compared to electrons, electrons can be considered to be in their ground state relative to the nuclei at any particular time, so the nuclei are considered

www.manaraa.com

fixed. Furthermore, each of these operator terms is considered in three dimensions, contributing to the difficulty of finding a solution, so as atoms are added to a quantum system, the complexity quickly increases. Finding an exact solution, the eigenvalue E and eigenfunction Ψ, to the time-independent Schrödinger equation becomes difficult to impossible for anything but the smallest systems, so solutions must be approximated by numerical methods. Throughout history, this issue of developing increasingly more exact methods of numerical approximation has been a major focus of quantum chemistry, and a focused explanation of that development can be found in Solid State Physics, by Neil W. Ashcroft and N. David Mermin[11].

An early step toward numerical approximation comes from the need to express the interaction between the electric fields of the electrons, which led to an application of the concept of a mean field. In this model, the complex electron-electron Coulombic interactions are replaced by the interaction between a single electron and a field that represents all of the other electrons. This field is treated as a smooth, negatively-charged probability density, ρ, commonly called electron density, with charge distribution

$$\rho(\vec{r}) = -e\sum_i |\psi_i(\vec{r})|^2 , \tag{3}$$

where the sum includes all occupied single-electron levels. Thus, the contribution to the field of any particular electron in the level ψ_i is

$$\rho_i(\vec{r}) = -e|\psi_i(\vec{r})|^2 , \tag{4}$$

and the potential energy of the single electron, U^{el}, in that field is

www.manaraa.com

$$U^{el}(\vec{r}) = -e\int \rho(\vec{r}\,')\frac{1}{|\vec{r}-\vec{r}\,'|}d\vec{r}\,'. \qquad (5)$$

The result of substituting these approximations, known collectively as the Hartree approximation, into the single-electron Schrödinger equation is the set of Hartree equations, each of which describes an occupied single-electron wave function, ψ_i:

$$-\frac{\hbar}{2m}\nabla_i^2\Psi + U^{ion}(\vec{r})\psi_i(\vec{r}) + \left[e^2\sum_j\int|\psi_j(\vec{r}\,')|^2\frac{1}{|\vec{r}-\vec{r}\,'|}d\vec{r}\,'\right]\psi_i(\vec{r}) = E\Psi, \qquad (6)$$

where U^{ion} is the potential term for the ions, or nuclei. The Hartree equations are solved iteratively in general, the first step being to substitute a potential form for the electron-electron interaction term, U^{el}, in brackets. Using this form, the system of equations are solved, and the resulting wave functions, ψ_i, are used to determine a new form for the U^{el} term. The process is repeated in iterations until there is no relevant change in the results from cycle to cycle, so the Hartree approximation is also referred to as the "self-consistent field approximation". What constitutes relevant change in energy is relative, but its absence is known as energy convergence.

The Hartree approximation is fundamentally flawed in two ways. One is that, by the nature of the approach, determining the way a particular electron configuration affects a single electron is precluded. The second is that it does not take into account the Pauli exclusion principle, which states that two electrons cannot be in the same quantum state, though this imperfection is less obvious. It stems from the fact that the Hartree equations approximate the full electron wave function in terms of a product of single-electron wave functions:

www.manaraa.com

$$\Psi(\vec{r}_1 s_1, \vec{r}_2 s_2, \ldots, \vec{r}_N s_N) = \psi_1(\vec{r}_1 s_1)\psi_2(\vec{r}_2 s_2)\ldots\psi_N(\vec{r}_N s_N), \quad (7)$$

where the single-electron functions ψ_i are spin orbitals, composed of a spatial function, $\phi_i(\vec{r})$, and one of two orthonormal spin functions, $\sigma_i(s)$, such that[12]

$$\psi_i = \phi_i(\vec{r})\sigma_i(s), \text{ where } (\sigma = \alpha, \beta). \quad (8)$$

As a simple product, the Hartree approximation for Ψ is commutative and violates the Pauli exclusion principle in two ways. Firstly, the Hartree scheme violates the fact that electrons are indistinguishable by assigning a single-electron function to one particular electron[12]. The second violation is that the full electron wave function must, according to Pauli, change sign whenever two of its arguments are exchanged, which is not the case with the traditional multiplication of the Hartree approximation. This means physically that the Hartree equations do not address anti-symmetry in electrons, thus they are limited to small, closed systems. This anti-symmetry flaw is addressed by what is known as the Hartree-Fock approximation, where Ψ is replaced with a linear combination of all the possible products of the form (7) found by permuting $\vec{r}_i s_i$. The terms are alternately multiplied by +1 and -1 to account for the requirement of the Pauli exclusion principle, leaving Ψ to take the following form[11]:

$$\Psi = \psi_1(\vec{r}_1 s_1)\psi_2(\vec{r}_2 s_2)\ldots\psi_N(\vec{r}_N s_N) - \psi_1(\vec{r}_2 s_2)\psi_2(\vec{r}_1 s_1)\ldots\psi_N(\vec{r}_N s_N) + \ldots \quad (9)$$

This can be rewritten as the determinant of an N x N matrix, known as a Slater determinant:

www.manaraa.com

$$\Psi(\vec{r}_1 s_1, \vec{r}_2 s_2, \ldots, \vec{r}_N s_N) = \begin{vmatrix} \psi_1(\vec{r}_1 s_1) & \psi_1(\vec{r}_1 s_1) & \ldots & \psi_1(\vec{r}_1 s_1) \\ \psi_1(\vec{r}_1 s_1) & \psi_1(\vec{r}_1 s_1) & \ldots & \psi_1(\vec{r}_1 s_1) \\ \vdots & \vdots & \ddots & \vdots \\ \psi_1(\vec{r}_1 s_1) & \psi_1(\vec{r}_1 s_1) & \cdots & \psi_1(\vec{r}_1 s_1) \end{vmatrix}, \tag{10}$$

where the signs are taken into account under the consideration that the sign of a determinant changes when any two rows or columns are interchanged.

At this point, the variational principle should be considered, whereby the energy associated with any trial wave function is an upper bound to the ground state energy corresponding to the ground state wave function[12]. In theory, the method employed to make use of the variation principle would be to search through all possible full electron wave functions to find that which minimizes the energy associated with it, and that wave function would be the ground state. Here, a possible wave function must be normalized, meaning that the probability of finding all N electrons anywhere in space is precisely unity. In the case of the Hartree-Fock approximation, the variational principle is applied to all Slater determinants with the goal of finding the member of that subset with the lowest, and thus approximate ground state, energy. Thus, using the variational principle along with the Slater determinant, the Hartree-Fock equations can be derived[11]:

$$-\frac{\hbar}{2m}\nabla_i^2\Psi + U^{ion}(\vec{r})\psi_i(\vec{r}) + U^{el}(\vec{r})\psi_i(\vec{r}) - \\ -\sum_j \int d\vec{r}\,' \frac{e^2}{|\vec{r}-\vec{r}\,'|}\psi_j^*(\vec{r}\,')\psi_i(\vec{r}\,')\psi_j(\vec{r})\delta_{s_i s_j} = \varepsilon_i \psi_i(\vec{r})\,. \tag{11}$$

This set of equations is a more generalized form of the Hartree equations, and it addresses the anti-symmetry problem by contributing an exchange term which prevents an electron from interacting with itself by canceling the electron-electron Coulombic interaction term

www.manaraa.com

when $i = j$. The addition of this term, while making the set of equations a more accurate approximation, makes finding an exact solution much more difficult than with the Hartree equations.

Another problem with the Hartree-Fock approach is what is known as the electron correlation energy, which is equal to the difference between the ground-state energy approximation resulting from Hartree-Fock and the true ground-state energy[12]. This correlation energy arises from the fact that the approximate wave function represented by a single Slater determinant can not correspond to the true full electron wave function, and by the variational principle must produce a corresponding energy that is higher than that of the true ground-state of the system. Electron correlation is essentially a result of the inaccuracy of the inter-electron repulsion term, which is due to averaging of the electrostatic interaction. This averaging, which is fundamental to Hartree-Fock, allows electrons to get closer to one another than they would physically. To correct for this interaction of electronic states, or configurations, the configuration interaction (CI) method was developed, in which the wave function is approximated by a linear combination Slater determinants constructed from spin orbitals. The linear coefficients are determined by diagonalizing the Hamiltonian within the subset of determinants particular to a system[30], so the full CI method is computationally expensive for anything but relatively small systems.

Due to its limitations, the Hartree-Fock equations can only be solved precisely when describing the case in which there is no periodic ionic potential, a free electron gas. Thus further development of numerical methods was required, and what followed formed the direct foundation for density functional theory.

www.manaraa.com

2.2, Density Functional Theory

The fundamental assumption upon which density functional theory, or DFT, is based is that the full electron wave function, Ψ, which describes N electrons each with one spin and three spatial variables which define it, can be approximated with a relatively simpler function, electron density[12]. This is a reasonable assumption because the Hamiltonian operator present in the time-independent Schrödinger equation (2) is defined by three variables (*N*, $\vec{R}$, and Z), each of which can be approximated, as will be shown, by electron density, $\rho(\vec{r})$. Firstly, the number of electrons, *N*, can be defined by the following integral:

$$\int \rho(\vec{r}_1) d\vec{r}_1 = N \,. \tag{12}$$

Secondly, the positions of the nuclei, $\vec{R}$, are detectable because the electron density has finite maxima that occur only at these locations due to their positive charge. Lastly, information regarding the nuclear charge, Z, is contained in the electron density according to the following expression:

$$\lim_{\vec{r}_{i,A}\to 0}\left[\frac{\partial}{\partial r} + 2Z_A\right]\bar{\rho}(\vec{r}) = 0 \,, \tag{13}$$

where $\vec{r}_{i,A}$ is the distance between electron i and nucleus A, Z_A is the charge of nucleus A, and $\bar{\rho}(\vec{r})$ is the spherical average of $\rho(\vec{r})$. The fact that the three defining variables of the Hamiltonian operator can be defined by the electron density is very useful, because, unlike the wave function, the electron density of a system is observable and can be measured via experiment. This does not alleviate the problem of actually finding a

www.manaraa.com

solution to the Schrödinger equation, but it does support the proposition that electron density can completely describe all of the molecular properties of a quantum system.

Modern density functional theory was established with the development of two theorems by Hohenberg and Kohn[13], and through them the above assumptions were justified. The first Hohenberg-Kohn theorem proves that an external potential, $U^{ext}(\vec{r})$, which fixes the Hamiltonian, is uniquely specified by the ground state electron density of the system. In the case of interest, this external potential is entirely defined by the attractive forces due to the nuclei. The result of this first theorem is that the full electron, ground state energy is a functional of the ground state electron density and can be expressed in the following way[12]:

$$E_0[\rho_0] = \int \rho_0(\vec{r}) U^{ext} d\vec{r} + T[\rho_0] + E^{el}[\rho_0]. \qquad (14)$$

Here the first term represents the potential energy due to the attraction between nuclei and electrons and is the only term that depends on the quantum system being described, i.e., depends on N, $\vec{R}$, and Z. The two other terms, the electron kinetic energy and electron-electron interaction operators, are independent of the system and are collectively known as the Hohenberg-Kohn functional, $F_{HK}[\rho_0]$. The second Hohenberg-Kohn theorem applies the variational principle to the connection between electron density and energy. It essentially states that, if supplied with the true ground state electron density of a particular system, the Hohenberg-Kohn functional will produce the ground state energy of that system[13]. Similarly to when it is applied in the Hartree-Fock approximation, the variational principle states that the energy associated with a trial electron density serves as an upper bound to the full electron, ground state energy. The combined result of the

www.manaraa.com

two theorems of Hohenberg and Kohn is that there is, in principle, a unique connection between the ground states of electron density and energy. Since the exact form of the Hohenberg-Kohn functional is unknown, the theorems did not establish a means to solve the Schrödinger equation but rather established the physical basis which permits the use of electron density as the principle variable to completely describe a quantum system[12]. It was with the development of the Kohn-Sham approach that a method for approximating the Hohenberg-Kohn functional was first proposed.

The work of Kohn and Sham essentially applied non-interacting single-electron wave functions, similar to those in the Hartree-Fock approach, to the Hohenberg-Kohn theorems[14]. These single-electron wave functions, or Kohn-Sham orbitals, made it possible to accurately calculate the relevant kinetic energy of a particular system, circumventing the difficulty of developing an explicit kinetic energy functional. This approach leaves out a portion of the kinetic energy, so Kohn and Sham introduced and exchange-correlation term, $E_{XC}[\rho(\vec{r})]$, such that

$$E_{XC}[\rho(\vec{r})] \equiv T_C[\rho(\vec{r})] + E_{si}[\rho(\vec{r})], \tag{15}$$

where T_C is the leftover element of kinetic energy and E_{si} describes an electron self-interaction correction[11]. Then, unlike the Hartree-Fock method, the Kohn-Sham method is exact except for the approximation of $E_{XC}[\rho]$, which contains those elements that are not precisely knowable. With the publication of the work of Kohn and Sham, the goal of modern density functional theory shifted towards the development of ever better approximations for the exchange-correlation functional.

www.manaraa.com

The first significant approximation for the exchange-correlation functional was the local density approximation, or LDA. Within this approach, whatever system is being studied is approximated to be a uniform electron gas, such that $\rho(\vec{r})$ is a finite constant and N and V, the volume of the gas, are considered to approach infinity. Physically, this describes a crystal of valence electrons and stationary positive cores, and in this system there is no net charge, since the cores, or nuclei, are approximated by a positive charge distribution on which the electrons move. This is the only system for which the exchange-correlation term in the Kohn-Sham approach is exactly calculable, and for this reason it has served as the foundation for all approximations that have followed. Under the LDA, $E_{XC}[\rho(\vec{r})]$ can be written in the following form:

$$E_{XC}^{LDA}[\rho] = \int \rho(\vec{r})\varepsilon_{XC}(\rho(\vec{r}))d\vec{r}\,, \tag{16}$$

where the exchange-correlation energy per single particle of $\rho(\vec{r})$, ε_{XC}, is combined with the probability of there being an electron at $\vec{r}$. In practice, it is convenient to develop an unrestricted form of an approximate functional which is expressed in terms of two spin densities, $\rho_{\uparrow}(\vec{r})$ and $\rho_{\downarrow}(\vec{r})$, representing up and down spin respectively, where

$$\rho_{\uparrow}(\vec{r}) + \rho_{\downarrow}(\vec{r}) = \rho(\vec{r})\,. \tag{17}$$

This unrestricted form is utilized because, in approximating a solution, using two variables rather than one can afford some additional flexibility. The unrestricted form of the local density approximation is the local spin-density approximation, or LSDA, and its exchange-correlation term is expressed in nearly the same form:

$$E_{XC}^{LSDA}[\rho_{\uparrow},\rho_{\downarrow}] = \int \rho(\vec{r})\varepsilon_{XC}(\rho_{\uparrow}(\vec{r}),\rho_{\downarrow}(\vec{r}))d\vec{r}\,. \tag{18}$$

www.manaraa.com

LDA and LSDA share a fundamental flaw concerning their application to problems of quantum systems, which is the following assumption on which they are based: The Kohn-Sham exchange-correlation term depends only very localized values of electron density. In almost any system of interest, electron density is not a constant, so the accuracy of local density approaches are limited. The development which followed was that of the generalized gradient approximation, or GGA, which takes into account the gradient of electron density at a particular point in space, $\nabla\rho(\vec{r})$. The exchange-correlation term of such an approximation thus takes the following general form:

$$E_{XC}^{GGA}[\rho_{\uparrow},\rho_{\downarrow}] = \int f(\rho_{\uparrow}(\vec{r}),\rho_{\downarrow}(\vec{r}),\nabla\rho_{\uparrow}(\vec{r}),\nabla\rho_{\downarrow}(\vec{r}))d\vec{r} \,. \tag{19}$$

Most modern DFT calculations model exchange-correlation interactions according to this general scheme.

Once a form for E_{XC} has been chosen, the Kohn-Sham method can be applied iteratively to find a numerical solution to the Schrödinger equation for a particular system. The iterations, which recall the Hartree-Fock method, begin with a trial electron density. Through the self-consistent field approximation, the trial density is used to calculate its associated energy, which in turn produces a new electron density. The cycle is repeated until there is convergence of energy, at which point that energy and the corresponding electron density are considered to be the ground state values for the system.

www.manaraa.com

2.3, Theoretical Methods

To utilize density functional theory to investigate the reactivity of aluminum iodide anions, two suites of code were used: Density of Montréal (deMon2k) and Naval Research Laboratory Molecular Orbital Library (NRLMOL). All presented results are the product of optimization in NRLMOL, though deMon2k was utilized for supplemental calculations which served to generate reasonable initial geometries to be used in NRLMOL. Both follow the Kohn-Sham approach, using a linear combination of Gaussian-type orbitals to express Kohn-Sham orbitals[15,18]. Summations of atomic orbitals, constructed from Gaussians, define the Kohn-Sham orbitals to be of the form

$$\psi_i(\vec{r}) = \sum_{\mu} c_{\mu i}\mu(\vec{r}), \tag{20}$$

where $\mu(\vec{r})$ is an atomic orbital, and $c_{\mu i}$ is the molecular orbital coefficient corresponding to μ. Electron density is similarly defined in terms of atomic orbitals, taking the following form:

$$\rho(\vec{r}) = \sum_{\mu,\nu} P_{\mu\nu}\mu(\vec{r})\nu(\vec{r}), \tag{21}$$

where $\nu(\vec{r})$ is another atomic orbital. Here $P_{\mu\nu}$ is the following element of the closed-shell density matrix:

$$P_{\mu\nu} = 2\sum_{i}^{occ} c_{\mu i}c_{\nu i}\ . \tag{22}$$

In both deMon and NRLMOL, the calculations that were performed to produce the presented results utilized the Perdew-Burke-Ernzerhof (PBE) exchange correlation functional, a GGA[17,20]

www.manaraa.com

$$E_{XC}^{PBE} = \int \rho(\vec{r}) \varepsilon_{XC}^{PBE}(r_s(\vec{r}), s(\vec{r}), \zeta(\vec{r})) d\vec{r}\,, \tag{23}$$

where $s(\vec{r}) = \dfrac{|\nabla\rho(\vec{r})|}{2(3\pi^2\rho(\vec{r}))^{1/3}\rho(\vec{r})}$ is the reduced density gradient, $\zeta(\vec{r}) = \dfrac{(\rho_\uparrow(\vec{r}) - \rho_\downarrow(\vec{r}))}{\rho(\vec{r})}$ is the spin-polarization, and $r_s(\vec{r}) = \left(\dfrac{4\pi\rho(\vec{r})}{3}\right)^{-1/3}$ is the Wigner Seitz radius, the local density parameter representing the approximate mean distance between electrons[16]. Then, ε_{XC}^{PBE} is the exchange-correlation energy per single electron of $r_s(\vec{r})$, $s(\vec{r})$, and $\zeta(\vec{r})$.

Most commonly in DFT calculation the basis sets is the set of Gaussian-type orbitals (GTOs) which represent each of the orbitals of the atoms, or the single-electron wave functions, in a system of interest. The basis sets utilized in deMon2k are its defaults, which are of the type known as Double-Zeta Valence Polarized, or DZVP[19]. Here, "double-zeta" means there are two basis functions representing each valence orbital instead of one to increase flexibility in calculation, and "polarized" means the basis set corrects for the case in which an electron strays into a d-orbital. In NRLMOL, the elements involved were each represented by the following basis sets::

Element (*Symbol*)	**Orbitals (*s*, *p*, *d*)**
Aluminum (*Al*)	*6*, *5*, *3*
Iodine (*I*)	*8*, 7, 5
Hydrogen (*H*)	*4*, *3*, *1*
Carbon (*C*)	*5*, *4*, *3*
Oxygen (*O*)	*5*, *4*, *3*

Basis sets used in NRLMOL calculations.

www.manaraa.com

Chapter 3, Results

The method followed in this study was generally twofold, first finding the ground state geometry for each of $Al_{13}I_x^-$ and $Al_{14}I_y^-$ ($x = 0-2$, $y = 2-4$). This was accomplished by optimizing all reasonable geometries for each cluster species[22,23] and taking that which had the lowest energy as the ground state. Secondly, the active sites of each cluster were investigated, which was accomplished in several steps. The first step was calculating the total energy at any potential active site for the cluster reacted with methanol with the O-H distance fixed, and then those energy values were compared. The potential sites were chosen according to the particular symmetry of the aluminum iodide cluster, but within these constraints every Al-Al and Al-I bond was investigated. When the lowest energy and the corresponding active site were identified for a particular cluster, one or two geometrically-varied additional sites were chosen, and these, along with the low energy case, were treated as the sites of interest. Once designated, these sites were further investigated to determine the following energy values for each: binding, transition state, and relaxation energies.

The binding energy, E_B, is the energy corresponding to the initial binding of the particular cluster and methanol with the O-H bond intact, as given by the following equation:

$$E_B = E_R - E_P, \tag{24}$$

where E_R is the energy of the reactants and E_P is the energy of the products. The value of the binding energy is an indicator as to how good of a Lewis acid a particular cluster

www.manaraa.com

is, because E_B is essentially a measure of the strength of the initial bond between the cluster and the oxygen of methanol. As E_B gets closer to zero energy, which corresponds to a separated cluster and molecule, the cluster is less reactive. The transition state energy, E_T, is found by increasing the O-H distance in methanol by .01 Angstrom increments until the maximum value, or saddle point, is discovered. This saddle point energy corresponds to the energy that is required to break the O-H bond. The relaxation energy, E_R, is associated with the final geometry of the system after reaction and is found by testing multiple possible outcomes and comparing them to find the lowest energy. Each of the three energy values is found relative to the combined energies of the reactants, which in the case of this study are always are $Al_{13}I_x^-$ or $Al_{14}I_y^-$ ($x = 0-2$, $y = 2-4$) and CH_3OH. E_B, E_T, and E_R are then compared graphically to determine the reaction pathway of a particular active site.

3.1, $Al_{13}I_x^-$, (x = 0 - 2)

To investigate the reactivity of clusters, it is first necessary to establish their ground state geometries. Thus, the geometries of the cluster anions in the $Al_{13}I_x^-$ series, where $x = 0-2$, were optimized to find that geometry which corresponded to the ground state energy for each molecular species, and the results are as follows:

www.manaraa.com

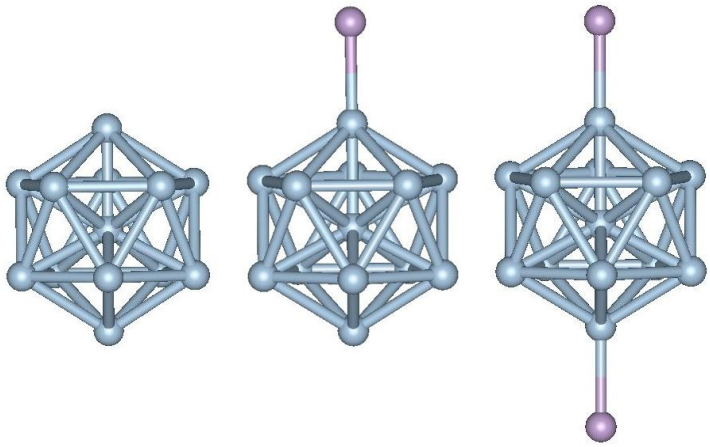

Fig. 6, Ground state geometries of, from left to right, Al_{13}^- , $Al_{13}I^-$, and $Al_{13}I_2^-$.

These ground state geometries are consistent with previous theoretical work[22,23]. The iodines seem to have a preference for establishment on opposite sides of the cluster. The energy required to remove an iodine, or the binding energy, from the ground state geometry of $Al_{13}I_2^-$ is 3.32 eV, while in the case that the two iodines are adjacent (Fig. 7) the binding energy is nearly an electronvolt less at 2.48 eV.

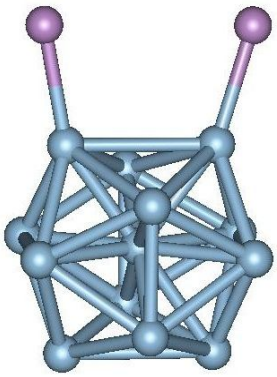

Fig. 7, Optimized geometries of $Al_{13}I_2^-$ with the iodine atoms on adjacent aluminums.

The extra stability of the ground state geometry of $Al_{13}I_2^-$ is a result of the second iodine binding to a half-filled active site on the opposite side of the cluster from the first, which

www.manaraa.com

maximizes the HOMO/LUMO gap. Note that the cluster maintains its icosahedral core after the addition of the iodine ligands.

From the geometries in Fig. 6, their electronic structure was determined (Fig. 8). The pure Al_{13}^- cluster anion shows a shell structure that corresponds closely to the jellium model, with orbitals that correspond to a $1s^2\ 1p^6\ 1d^{10}\ 2s^2\ 2p^6\ 1f^{14}$ electronic structure.

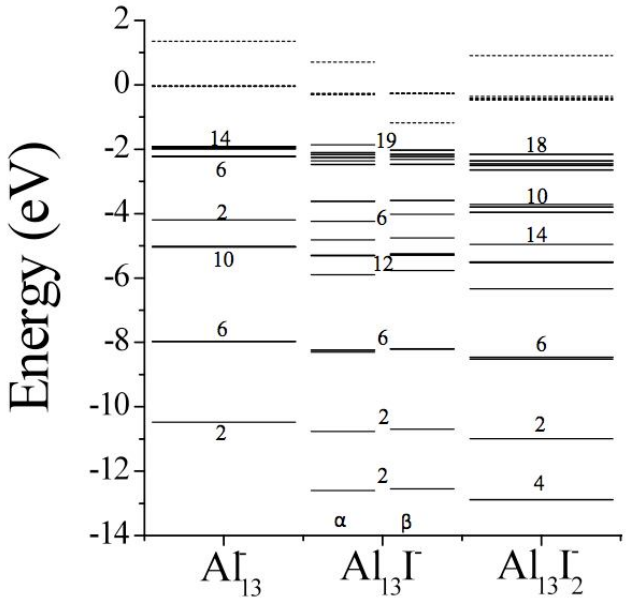

Fig. 8, Electronic structures of the $Al_{13}I_x^-$ series.

Each time an iodine atom is introduced, a covalent bond forms causing the shells to split, though the overall shell structure remains visible. Since $Al_{13}I^-$ has an odd number of electrons, there is an unpaired electron, hence the α and β spin channels have different energies, though the energy difference between the two is very small. For Al_{13}^- and $Al_{13}I_2^-$ the band gap between the highest occupied and the lowest unoccupied molecular orbitals (HOMO, LUMO) is between 1.90 and 1.70 eV, and in the case of $Al_{13}I^-$ this HOMO/LUMO gap is 0.69 eV. The second lowest unoccupied molecular orbital, or LUMO+1, remains relatively high in energy for all three clusters. The high energy of the LUMOs for Al_{13}^- and $Al_{13}I_2^-$ along with the high lying LUMO+1 for $Al_{13}I^-$ suggest that

www.manaraa.com

each of these clusters is likely to be a poor Lewis acid. We are interested in the LUMO+1 of $Al_{13}I^-$ in particular because Lewis acidity requires the acceptance of two electrons, and the high filled HOMO/LUMO states in $Al_{13}I^-$ can accept only one electron.

Due to its high symmetry, all potential active site on Al_{13}^- is geometrically equivalent, and so this cluster has only one reaction pathway:

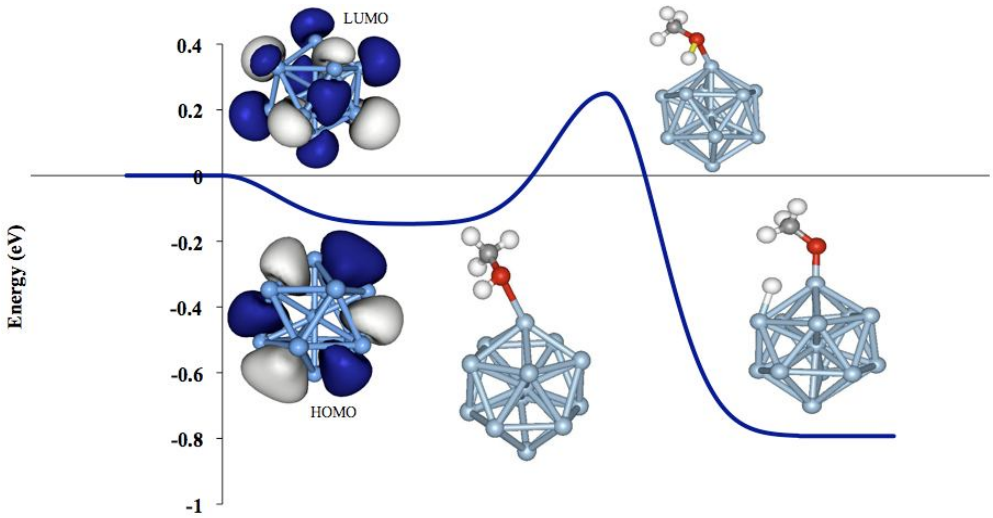

Fig. 9, Reaction pathway for Al_{13}^-.

Basic reaction pathways such as this can be considered to have four distinct sections, each corresponding to a geometry and corresponding energy level. The first section is of zero energy and coincides with the ground state geometry before any reaction has taken place. The second section is the negative E_B, and the third is the transition state energy, E_T. E_T can be positive or negative depending on reactivity, but it will always be higher than the binding energy. The fourth section corresponds to the final state, E_R. In this study, each of the aforementioned sections is graphically accompanied by its relevant geometry, and the ground state geometry is depicted with HOMO and LUMO charge densities. Since, in Fig. 9, E_T is a positive value, Al_{13}^- is a relatively nonreactive cluster.

www.manaraa.com

This is to be expected because, since it has a nearly spherically symmetric, icosahedron geometry, its charge density is considered nearly constant so that no site on the cluster may be considered an active site. This finding is consistent with related work with aluminum cluster anions and H_2O[6] and a reactivity study of pure Al_n^- clusters with methanol, both finding Al_{13}^- to be resistant to etching.

For $Al_{13}I^-$, it was determined that the active site that corresponds with the lowest energy is at the aluminum atom on the opposite side of the cluster with respect to the iodine. This site is also the location of the HOMO, and as such the hydrogen of the O-H bond is expected to bond there. This expectation stems from the fact that, in methanol, the HOMO is on the oxygen, and the LUMO is on the hydrogen (Fig. 10). Since a HOMO acts as an electron donor and a LUMO as an electron receiver, the HOMO of methanol will be attracted to the LUMO of the aluminum iodide cluster.

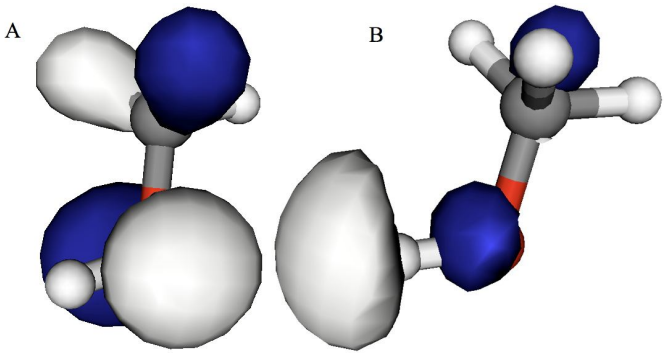

Fig. 10, HOMO (A) and LUMO (B) charge densities for CH_3OH.

The following (Fig. 11) are reaction pathways for the three cases: (A) when hydrogen is at the aluminum site opposite the iodine, (B) when oxygen is at the same site, and (C) when oxygen is at the aluminum atom bonded to the iodine.

www.manaraa.com

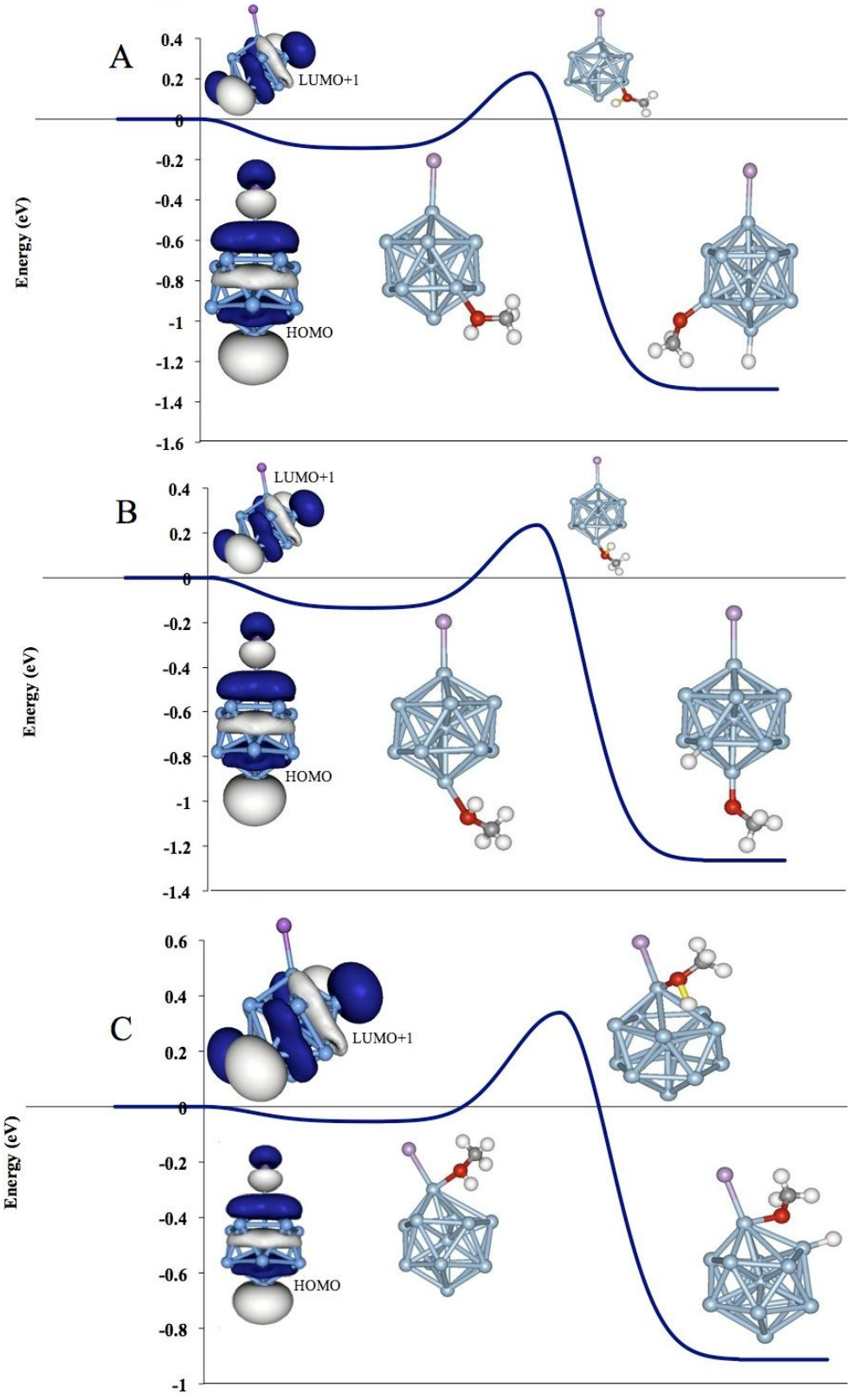

Fig. 11, Reaction pathways for $Al_{13}I^-$.

www.manaraa.com

Note that, since $Al_{13}I^-$ has an odd number of electrons, LUMO+1 is presented instead of LUMO. The transition state energies for Fig. 11A and Fig. 11B are nearly the same, 0.228 and 0.235 eV respectively, while E_T for Fig. 11C is a tenth of an electronvolt higher at .339 eV. The expectation was that the induced HOMO would have a larger effect on increasing the reactivity, but it has only reduced the transition state by 7 meV, making the effect close to negligble. Since the E_T values are positive and E_B is near zero in each case, the conclusion is that $Al_{13}I^-$ is a poor Lewis acid and is nonreactive. Thus, in an interesting result, the finding that $Al_{13}I^-$ is nonreactive does not seem to correlate with the low HOMO/LUMO gap of the cluster, and the addition of the iodine ligands does not induce reactivity in these clusters.

In the case of $Al_{13}I_2^-$, the lowest active site is perpendicular the aluminum-iodide bond such that the oxygen and hydrogen of the O-H bond are both adjacent to the same aluminum bonded to an iodine. As with $Al_{13}I^-$, the position of this site was consistent with the HOMO/LUMO model of methanol. The reaction pathway associated with this active site is in Fig. 12A. The reaction pathway for the case in which the O and H are adjacent to the different aluminums, each bonded to an iodine, is in Fig. 12B.

www.manaraa.com

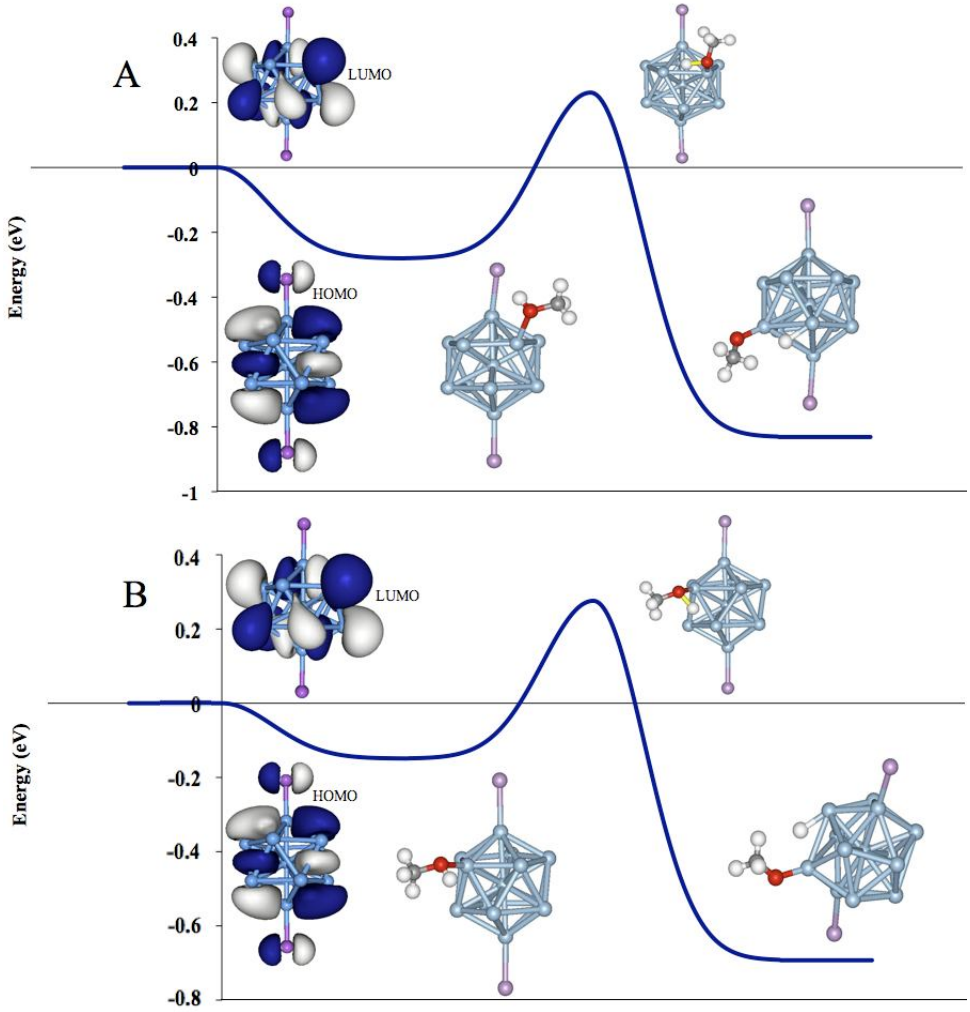

Fig. 12, Reaction pathways for $Al_{13}I_2^-$.

The binding energy for 12A is about 0.13 eV higher than 12B, pointing to the conclusion that it is a slightly better Lewis acid site, but the transition state energies are 0.231 and 0.276 eV for 12A and 12B respectively, these positive values once again suggesting nonreactivity.

One motivation for this project is identifying methods by which the reactivity may be increased by the addition of ligands. To study the effect on reactivity of moving a ligand, the geometry in Fig. 12B is altered such that the iodines are bound to adjacent

www.manaraa.com

aluminum atoms (Fig. 7) and the active site remains in the same location relative to the iodine that has not moved.

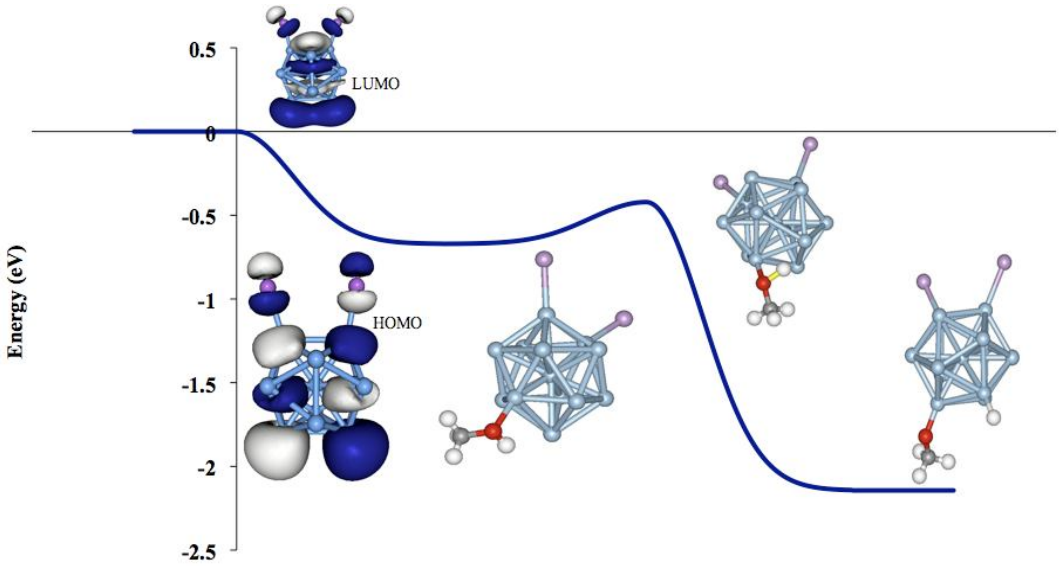

Fig. 13, Reaction pathways for $Al_{13}I_2^-$ with adjacent iodides.

Here, the rearrangement of the geometry of the cluster, with no additional charge added to the system, shifts the charge density in such a way as to make the system reactive. This is concluded because the transition state energy is a negative value, $E_T = -0.421\,\text{eV}$. Also, a large binding energy relatively far from zero is expected when a cluster is reactive, and this is the case here, where $E_B = -0.671$. The HOMO and LUMO charge density are both located primarily on the two atoms opposite the iodines, resulting in the formation of an effective complementary active site. In Fig. 14, the electronic structure of $Al_{13}I_2^-$ in its ground state (Fig. 8) is juxtaposed with the electronic structure of $Al_{13}I_2^-$ with iodines on adjacent aluminums.

www.manaraa.com

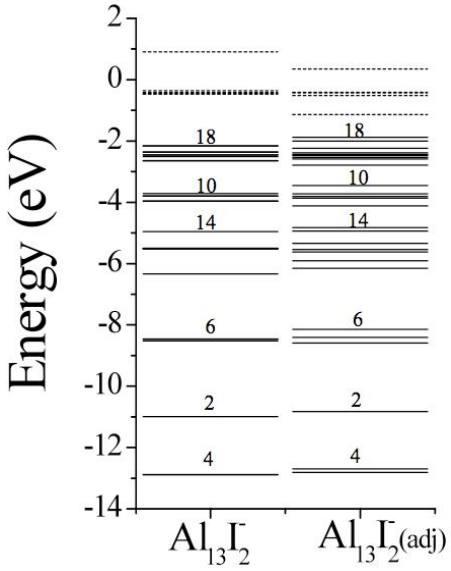

Fig. 14, Electronic structures of the "ground state" (left) and "adjacent iodine" (right) versions of $Al_{13}I_2^-$.

Notice that the difference in geometry disrupts the symmetry of the charge density of the cluster, resulting in a significant split of the electron shells. From the ground state geometry to the geometry with adjacent iodines, the HOMO/LUMO gap decreases from 1.697 to 0.701 eV, a difference of almost a full electronvolt. Also, the LUMO level is drastically lower in the case of adjacent iodine atoms, suggesting that this geometry is much better Lewis acid site. It must be noted that this reactive geometry is not associated with the ground state energy of $Al_{13}I_2^-$, so it is not expected to be a common isomer of the cluster. However, it does point to the role that geometry and the associated electron density plays in the reactivity mechanism of a cluster, and proves the principle that the addition of ligands may introduce active sites resulting in a method of activating the clusters.

www.manaraa.com

The theoretical study of the reactivity of $Al_{13}I_x^-$ ($x = 0 - 2$) with methanol leads to the conclusion that these cluster species are nonreactive in their ground state, which may be a result of the effect of a relatively high level of symmetry of charge density due to their strong icosahedral aluminum cores. Within the confines of ground state geometry, no potential active site showed reactivity, which suggests this series of clusters is fundamentally stable. The only case which resulted in reactivity was that of the non-ground state geometry of $Al_{13}I_2^-$, in which the iodines were not opposite one another.

3.2, $Al_{14}I_y^-$, (y = 2 - 4)

As with the $Al_{13}I_x^-$ series, the necessary preliminary step in the investigation of $Al_{14}I_y^-$ ($y = 2 - 4$) was to establish the relevant ground state geometries. Thus, the geometries in Fig. 15 correspond to the ground state energies of the molecular species of interest and are consistent with other theoretical calculations[22,23]. The geometric motif that is common to the clusters of the form $Al_{14}I_y^-$ is an icosahedral core consisting of thirteen aluminum atoms, with a single aluminum adatom on its surface. Without exception, this adatom is bound to an iodine. In this series, any additional iodine atoms bond on the side of the cluster that is opposite the aluminum adatom.

www.manaraa.com

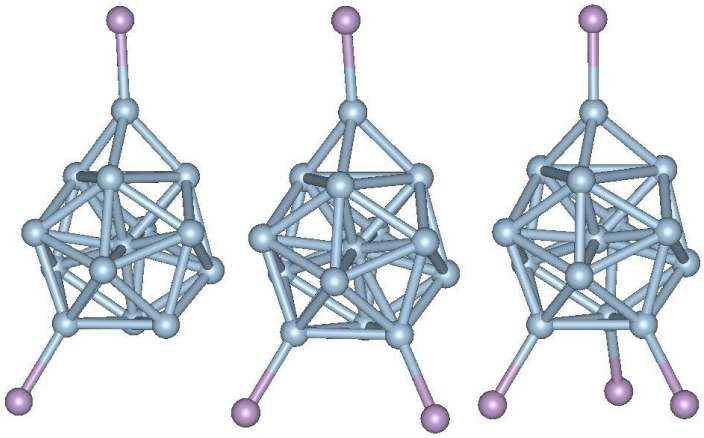

Fig. 15, Ground state geometries of, from left to right, $Al_{14}I_2^-$, $Al_{14}I_3^-$, and $Al_{14}I_4^-$.

These clusters lack the symmetry that serves as the geometric basis for the $Al_{13}I_x^-$ series, which is reflected in the corresponding electronic structures:

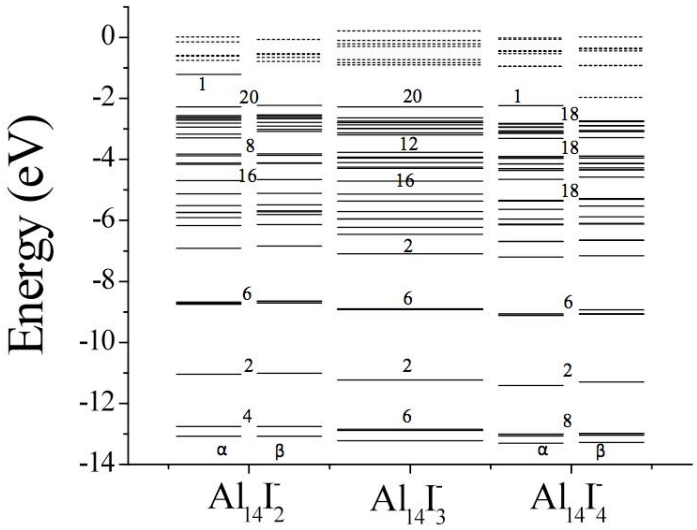

Fig. 16, Electronic structures of $Al_{14}I_y^-$ series.

Unlike the electronic structures of the $Al_{13}I_x^-$ series, these show much more splitting of electron shells resulting from their asymmetry and the bonding with iodine. In other words, clusters that constitute the $Al_{14}I_y^-$ series have electronic structures that show some remnants of an electron shell, but the iodines have significantly smeared the electronic

www.manaraa.com

shells in the top half of the electronic structures. Here, as with $Al_{13}I^-$, clusters with odd numbers of electrons, i.e., $Al_{14}I_2^-$ and $Al_{14}I_4^-$, experience degeneracy and have α and β structures. The HOMO/LUMO gaps for y = 2, 3, 4, including degeneracy, are 0.428, 1.374, and 0.274 eV respectively, suggesting that $Al_{14}I_3^-$ might be less reactive than $Al_{14}I_2^-$ or $Al_{14}I_4^-$. An important characteristic of the clusters in this series is that in, each case, the LUMO is significantly lower in energy than the $Al_{13}I_x^-$ series. This leads to the consideration that the $Al_{14}I_y^-$ series cluster anions might be good Lewis acids, which could contribute to reactivity. To investigate the reactivity of $Al_{14}I_y^-$ ($y = 2-4$) with methanol, the same approach is taken as outlined in the introduction to this chapter.

In the case of $Al_{14}I_2^-$, the lack of symmetry meant the existence of several more potential active sites than in the highly symmetric $Al_{13}I_x^-$ series, and the energy at each site was calculated and compared. From those potential sites, three active sites were investigated further (Fig. 17): (A) the lowest energy site, where the methanol oxygen is located at the aluminum adatom and the hydrogen at the adjacent aluminum in the direction of the second iodine atom, (B) the case where the oxygen is located at the iodine not bonded to the adatom, and (C) the case where the oxygen and hydrogen are located on two aluminum atoms, neither of which is bonded to an iodine. This third case is hereto referred to as “all-metal”.

www.manaraa.com

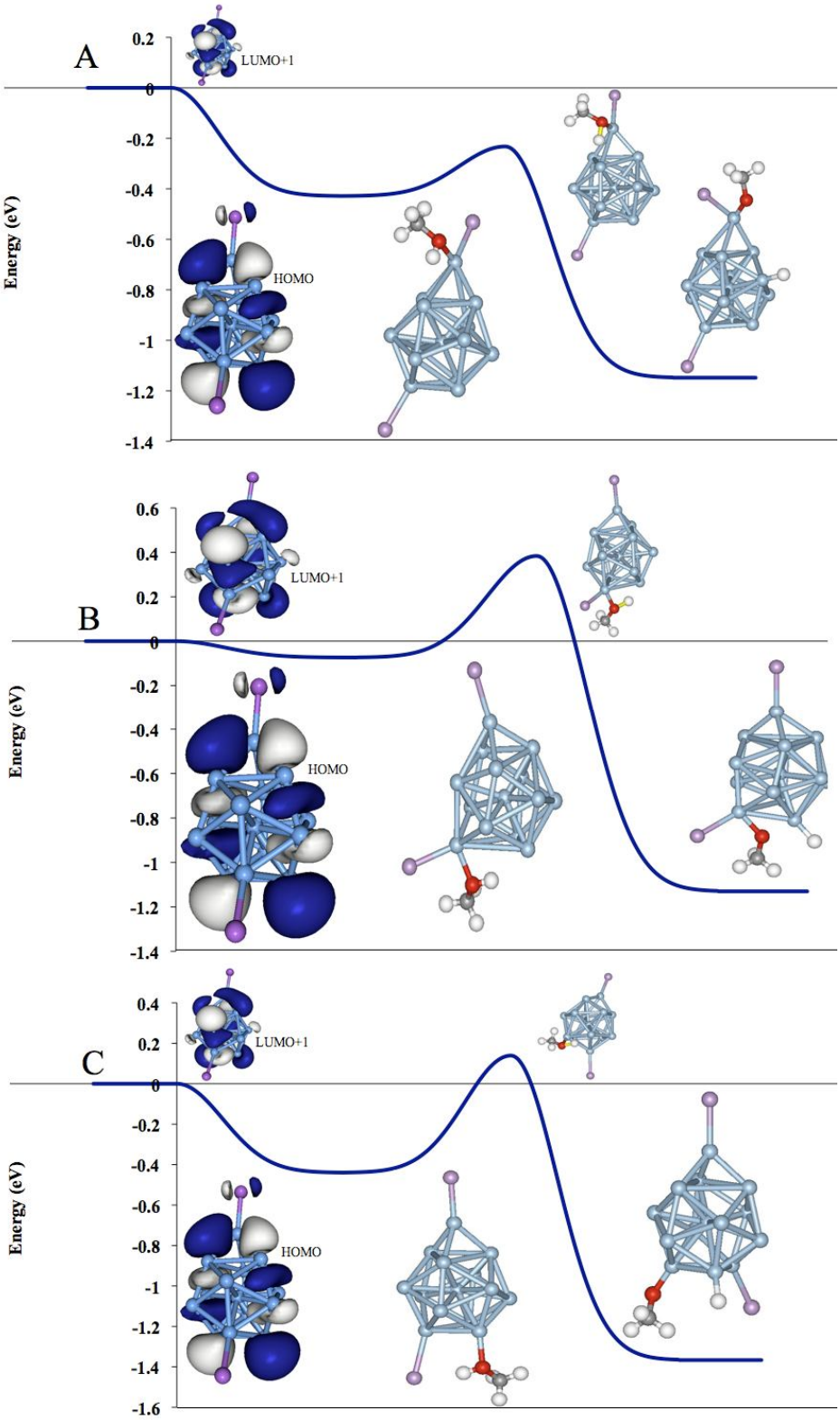

Fig. 17, Reaction pathways for $Al_{14}I_2^-$.

www.manaraa.com

Of the three potential active sites that were investigated, only the lowest energy site, with oxygen at the aluminum adatom, proved reactive. This is apparent considering the negative transition state energy at that site (-0.232 eV) and is supported by the relatively large negative value for the binding energy (-0.429 eV). By comparison, the case in which methanol binds to the aluminum bonded to the other iodine has an associated E_T of 0.384 eV and a binding energy very close to zero (-0.074 eV), thus showing to being nonreactive. The all-metal case is also nonreactive, though with a smaller transition state energy (0.139 eV) than that of the second site and a binding energy even larger than that of the most active site (0.440 eV). In the case of Fig. 17C, the indication is that the site might serve as a good Lewis acid, but the transition state barrier is too high in energy to overcome for a reaction to take place..

As in the previous case, the relative asymmetry of the cluster anion $Al_{14}I_3^-$ required that several potential active sites be investigated and their energies compared. From those potential sites, three active sites were investigated further (Fig. 18), and they follow the same scheme outlined for $Al_{14}I_2^-$. The first active site (A) is the lowest energy site, where the methanol oxygen is located at the aluminum adatom. The second site (B) is the case where the oxygen is located at a non-adatom aluminum bonded to an iodine, and the last site (C) is all-metal.

www.manaraa.com

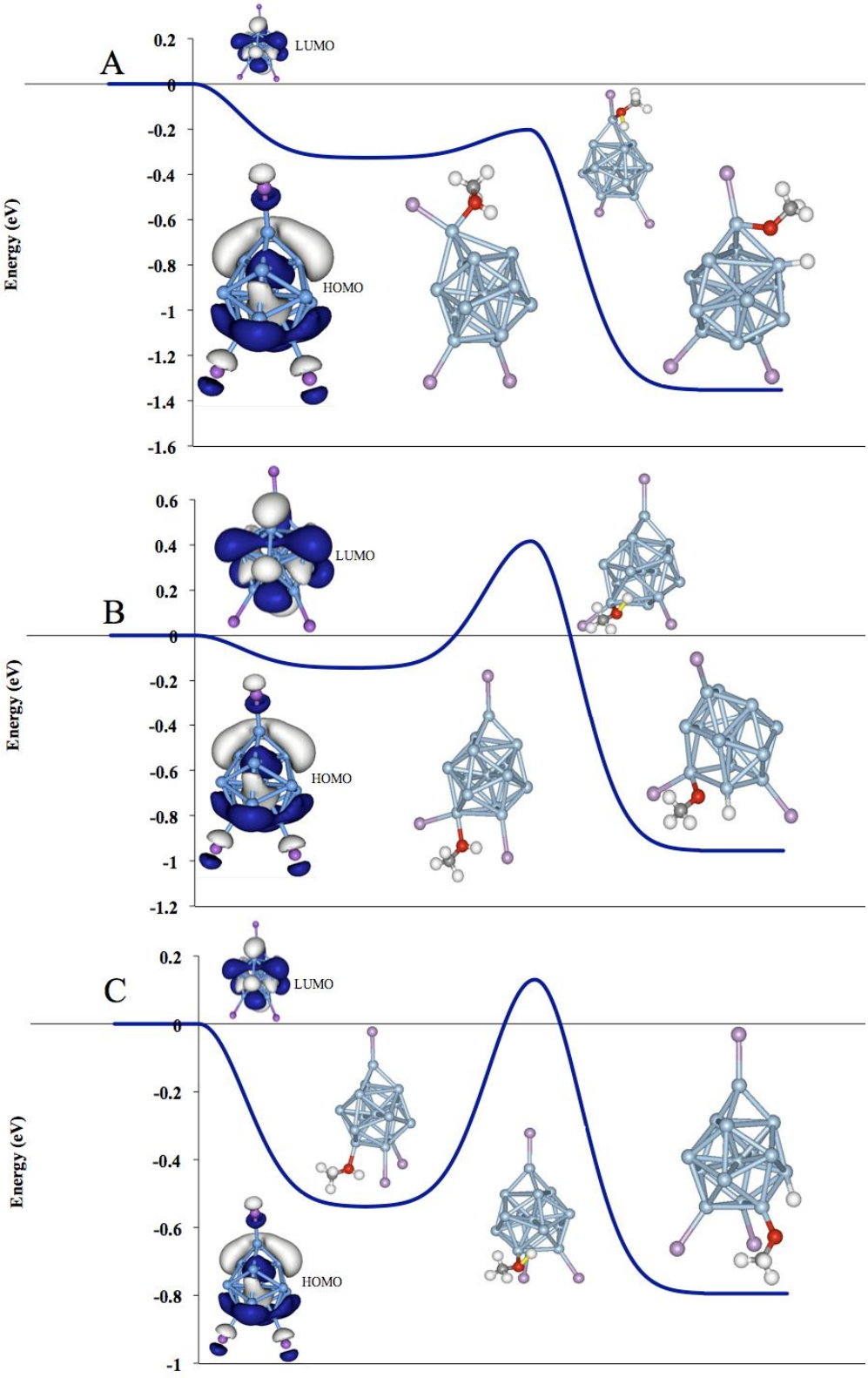

Fig. 18, Reaction pathways for $Al_{14}I_3^-$.

www.manaraa.com

As in the case of $Al_{14}I_2^-$, only the lowest energy site, with oxygen at the aluminum adatom, proved reactive. In this case, there is a negative transition state energy at (-0.203 eV) and a relatively large negative value for the binding energy (-0.326 eV). Again, the second case, in which methanol binds to a non-adatom aluminum bonded to an iodine, is nonreactive. That site has an associated E_T of 0.416 eV and a very low binding energy of -0.144 eV. In the all-metal case the site is nonreactive, with a transition state energy of 0.130 eV and a large binding energy of -0.539 eV. Again, this binding energy suggests a good Lewis acid, with too high a transition state energy to overcome.

A study of the cluster anion $Al_{14}I_4^-$ is currently underway at the time of this report, and the preliminary data appears to follow the trend established by $Al_{14}I_2^-$ and $Al_{14}I_3^-$. The binding, transition state, and relaxation energies are being investigated for three potential active sites of the same type as those in the cases above. The following set of reaction pathways (Fig. 19) was created for $Al_{14}I_4^-$, but, since the forces for some geometries have not fully converged, only approximate energies are given in some cases. For each of the reaction pathways, only those calculations which have converged are represented by geometries. The reaction energies for all three potential active sites and the binding energy for the site opposite the adatom have been approximated, but all other energies are the result of completed iterative calculation:

www.manaraa.com

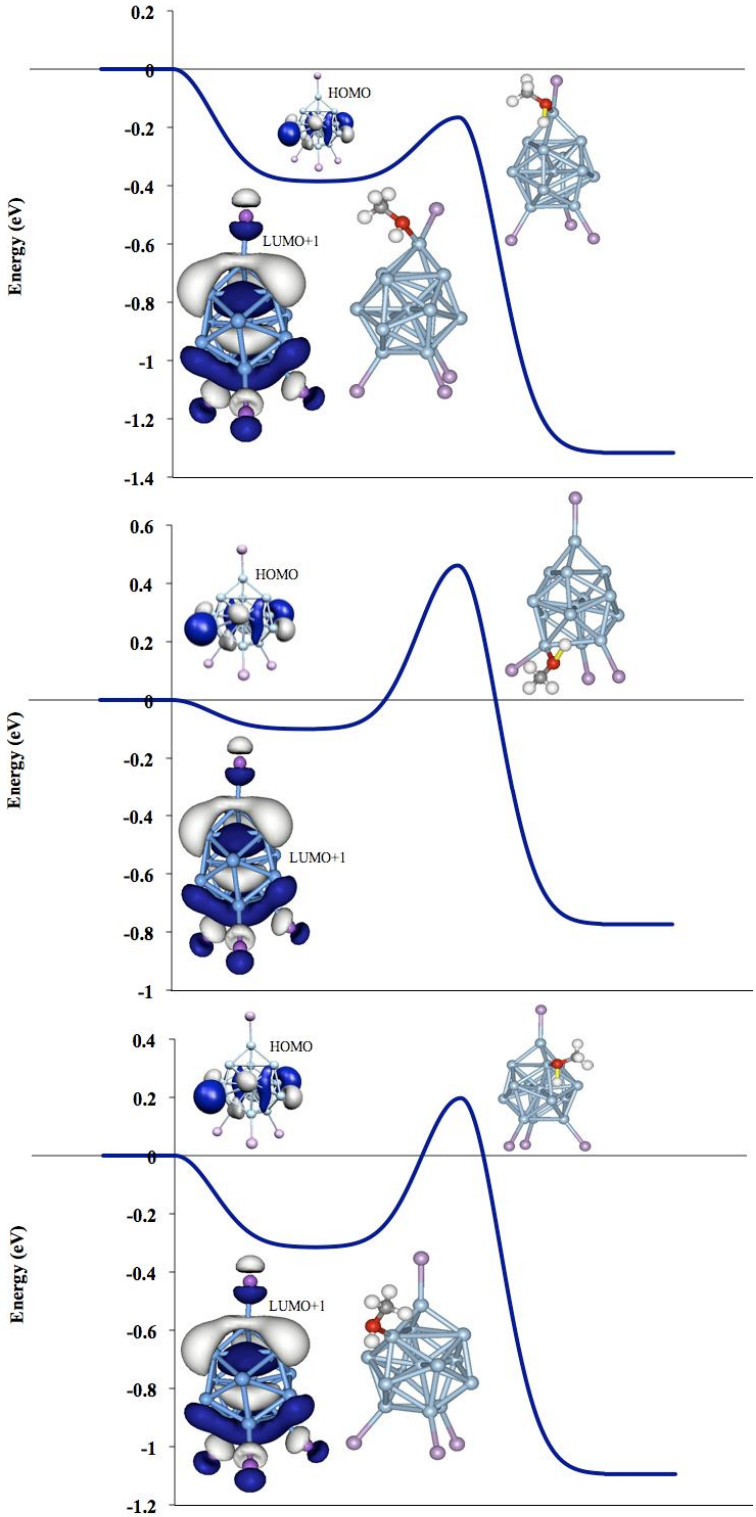

Fig. 19, Reaction pathways for $Al_{14}I_4^-$. For those geometries not pictured, the corresponding energy value has been approximated based on ongoing calculations.

www.manaraa.com

Again, the ground state site is at the aluminum adatom bonded to an iodine atom. This site has a large negative E_B of -0.385 eV, suggesting it is a strong Lewis acid, and a negative E_T of -0.166 eV, showing it is reactive. Thus, the lowest energy active site of $Al_{14}I_4^-$, as with $Al_{14}I_2^-$ and $Al_{14}I_3^-$, is reactive. The potential site opposite the aluminum adatom, according to the available results, appears to be nonreactive in the same way as the corresponding sites on $Al_{14}I_2^-$ and $Al_{14}I_3^-$. This is based on its positive transition state energy of 0.461 eV. Lastly, the all-metal potential site also seems to follow the trend set by other molecular species in the $Al_{14}I_y^-$ series in that, in spite of a large negative binding energy (-0.315 eV), there is a positive transition state energy of 0.197 eV, meaning the site is nonreactive.

In comparing the sites for each species in the $Al_{14}I_x^-$ series, the trends are apparent. For one, the all-metal sites are consistently nonreactive, supporting the notion that it is indeed the addition of iodide to the adatom site that makes Al_{14}^- reactive. Secondly, the aluminum adatom bonded to an iodine makes a good Lewis acid, while an aluminum atom on the icosahedral part of the cluster that is bonded to an iodine is decisively nonreactive.

It is interesting to consider that an iodine on a particular aluminum atom induces reactivity while an iodine on another does not. When an atom of iodine is bound to an aluminum atom, it draws charge from the aluminum. The result is that the iodines have a relatively large negative charge and the attached aluminums have a positive charge, which serves as a Lewis acid and attracts the methanol. One explanation why the iodine bonded to the aluminum adatom induces a reaction whereas another iodine-aluminum pair is nonreactive is geometric. The angle formed by the iodine opposite the adatom is

www.manaraa.com

more acute and therefore is inopportune for methanol to bind, while the adatom projects its iodine away from the cluster, facilitating the methanol binding and reactivity. Thus, adatoms are made more reactive when bonded to a ligand. These results reveal that, even in clusters with ligands, the concept of closing a geometric shell remains important. Electronegative ligands bonded to adatom defects result in reactive ligated clusters, while ligands on an icosahedral shell result in decreased reactivity.

www.manaraa.com

Chapter 4, Conclusions

Size selective reactivity has been observed in pure aluminum cluster anions as a result of Lewis acid and base pairs. Using this as a starting point, the goal of this study has been to explore how reactivity is affected with the addition of one or more ligand, which may induce complementary active sites on the surface of the metal clusters. To study this, a theoretical investigation was undertaken on $Al_{13}I_x^-$ and $Al_{14}I_y^-$ ($x = 0-2$, $y = 2-4$) and their reactivity with methanol. The hypothesis was that iodine can induce a Lewis base site on the opposite side of the cluster, which may enhance reactivity.

In results that are consistent with preliminary experimental data, it was found that the $Al_{13}I_x^-$ series has a large energy barrier with respect to the cleavage of the O-H bond of methanol. The clusters of the series act as an extremely poor Lewis acids, and as a result, these clusters are relatively inert to methanol etching. However, it was found that by placing both iodines on adjacent aluminum atoms, a strong Lewis acid-Lewis Base pair is created on the opposite side of the cluster, resulting in a highly reactive isomer of $Al_{13}I_2^-$. This serves as a proof of principle that the use of unbalanced ligand may induce active sites in metallic clusters. Unfortunately, considering that this is a high energy isomer, experimental verification may not be difficult. The reactivity of the ground state geometries has been experimentally verified, as Al_{13}^- and $Al_{13}I_2^-$ are both resistant of methanol etching in experiments, and $Al_{13}I^-$ has not been experimentally studied, although we predict that it will also be found to be inert.

www.manaraa.com

On the other hand, the $Al_{14}I_y^-$ series has a low barrier and is expected to react rapidly with methanol. The series is found to be most reactive at an aluminum adatom that is bound to an iodine due to the iodine extracting charge from the aluminum cluster creating a strong Lewis acid site. Sites which are all-metal and icosahedral sites which are bound to iodine are resistant to methanol reactivity. This demonstrates that the concept of geometric shell closure is still important in ligated clusters, as adatoms are made more reactive when ligated. These results reveal the effects of ligands on quantum confined metal clusters may produce unexpected reactivity, and motivate further studies on the stability of ligated clusters.

www.manaraa.com

List of References

[1] M. Campbell, "Magnetic 'Superatoms' Promise Tuneable Materials"; New Scientist (2009)

[2] A.W. Castleman, Jr., S.N. Khanna, "Clusters, Superatoms, and Building Blocks of New Materials", J. Phys. Chem., **113**, 2664 (2009)

[3] R.E. Leuchtner, A.C. Harms, A.W. Castleman, Jr., J. Chem. Phys., **91**, 2753 (1989)

[4] J.U. Reveles, S.N. Khanna, P.J. Roach, A.W. Castleman, Jr., "Multiple Valence Superatoms", PNAS, **103**, 18405 (2006)

[5] S.A. Claridge, A.W. Castleman, Jr., S.N. Khanna, C.B. Murray, A. Sen, P.S. Weiss, "Cluster-Assembled Materials", ACS NANO, **3**, 244 (2009)

[6] P.J. Roach, W.H. Woodward, A.W. Castleman, Jr., A.C. Reber, S.N. Khanna, "Complementary Active Sites Cause Size-Selective Reactivity of Aluminum Cluster Anions with Water", Science, **323**, 492 (2009)

[7] K. Clemenger, "Elipsoidal Shell Structure in Free-Electron Metal Clusters", Phys. Rev. B**, 32**, 1359 (1985)

[8] P. Muller, "Glossary of Terms Used in Physical Organic Chemistry", Pure Appl. Chem., **66**, 1077 (1994)

[9] A. W. Castleman Jr., K. G. Weil, S. W. Sigsworth, R. E. Leuchtner, R. G.. Keesee, "Considerations of the Rates and Lifetimes of Intermediate Complexes

www.manaraa.com

for the Association of Various Ligands to Metal Ions: Ag^+ and Cu^+", J. Chem. Phys., **86**, 3829 (1987)

[10] D.E. Bergeron, P.J. Roach, A.W. Castleman Jr., N.O. Jones, S.N. Khanna, "Al Cluster Superatoms as Halogens in Polyhalides and as Alkaline Earths in Iodide Salts", Science, **307**, 231 (2005)

[11] N.W. Ashcroft, N.D. Mermin, Solid State Physics, College ed., Thomson Learning, Inc., (1976)

[12] W. Koch, M.C. Holthausen. A Chemist's Guide to Density Functional Theory, 2nd ed., Weinheim, Germany: Wiley-VCH, (2001)

[13] P. Hohenberg, W. Kohn, "Inhomogeneous Electron Gas", Phys. Rev., **136**, B864 (1964)

[14] W. Kohn, L.J. Sham, "Self Consistent Equations Including Exchange and Correlation Effects", Phys. Rev., **140**, A1133 (1965)

[15] A.M. Köster, P. Calaminici, S. Escalante, R. Flores-Moreno, A. Goursot, S. Patchkovskii, J.U. Reveles, D.R. Salahub, A. Vela, The deMon User's Guide, Version 1.1 (2004)

[16] J.P. Perdew, M. Ernzerhof, A. Zupan, and K. Burke, "Nonlocality of the Density Functional for Exchange and Correlation: Physical Origins and Chemical Consequences", J. Chem. Phys., **108**, 1522 (1998)

www.manaraa.com

[17] J.P. Perdew, K. Burke, M. Ernzerhof, "Generalized Gradient Apprioximation Made Simple", Phys. Rev. Lett., **77**, 3865 (1996)

[18] T. Baruah. "NRLMOL." The University of Texas at El Paso, 06 Feb 2008. Web. 06 Feb 2011. <http://quantum.utep.edu/nrlmol/nrlmol.html >.

[19] N. Godbout, D.R. Salahub, J. Andzelm, E. Wimmer, "Optimization of Gaussian-Type Basis Sets for Local Spin Density Functional Calculations. Part I. Boron Through Neon, Optimization Technique and Validation", Can. J. Phys., **70**, 560 (1992)

[20] M. Ernzerhof, G. Scuseria, "Assessment of the Perdew-Burke-Ernzerhof Exchange-Correlation Function", J. Chem. Phys., **110**, 5029 (1999)

[21] S. Chiodo, N. Russo, and E. Sicilia, "Newly Developed Basis Sets for Density Functional Calculations", J. of Computational Chem., **26,** 175 (2005)

[22] R. Fournier, "Trends in Energies and Geometric Structures of Neutral and Charged Aluminum Clusters", J. of Chem. Theory and Computation, **3**, 921 (2007)

[23] B.K. Rao, P. Jena, "Evolution of the Electronic Structure and Properties of Neutral and Charged Aluminum Clusters: A Comprehensive Analysis", J. Chem. Phys, **111**, 1890 (1999)

[24] A.C. Reber, S.N. Khanna, P.J. Roach, W.H. Woodward, A.W. Castleman, Jr.,

www.manaraa.com

"Spin Accommodation and Reactivity of Aluminum Based Clusters with O_2", J. Am. Chem. Soc., **129**, 16098 (2007)

[25] N. Drebov, R. Ahlrichs, "Structures of Al_n, its anions and cations up to $n = 34$: A Theoretical Investigation", J. Chem. Phys., **132**, 164703 (2010)

[26] F. Chuang, C.Z. Wang, K.H. Ho, "Structure of Neutral Al_n ($2 \le n \le 23$): Genetic Algorithm Tight-Binding Calculations", Phys. Rev. B, **73**, 125431 (2006)

[27] J.U. Reveles, P.A. Clayborne, A.C. Reber, S.N. Khanna, K. Pradhan, P. Sen, M.R. Pederson, "Designer Magnetic Superatoms", Nature Chem., **1**, 310 (2009)

[28] A.C. Reber, S.N. Khanna, A.W. Castleman, Jr., "Superatom Compounds, Clusters and Assemblies: Ultra Alkali Motifs and Architectures", J. Am. Chem. Soc., **129**, 10189 (2007)

[29] D.M. Cox, D.J. Trevor, R. L. Whetten, A. Kaldor, "Aluminum Clusters: Ionization Thresholds and Reactlvtty toward Deuterium, Water, Oxygen, Methanol, Methane, and Carbon Monoxide", J. Phys. Chem., **92**, 421 (1988)

[30] C.D. Sherril, T.D. Crawford, E.F. Valeev, M.L. Abrams, R.A. King, A. Ringer, The PSI3 User's Manual, Version 3.4.0 (2009)

[31] A.M. Köster, P. Calaminici, S. Escalante, R. Flores-Moreno, A. Goursot, S. Patchkovskii, J.U. Reveles, D.R. Salahub, A. Vela, demon 2003, NRC, Canada

www.manaraa.com